

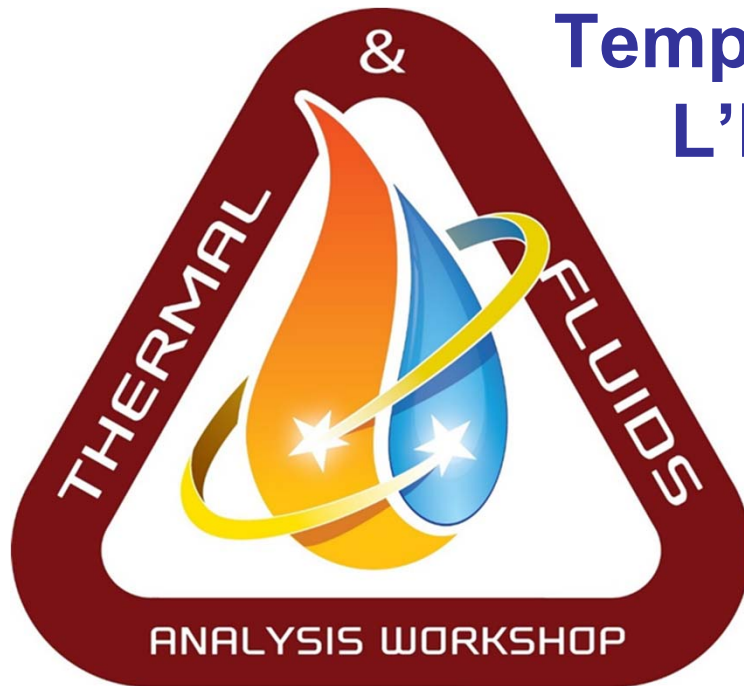


## Review of MLI Behavior at Low Temperatures and Application to L'Ralph Thermal Modeling

Daniel Bae

Juan Rodriguez-Ruiz

Presented By  
Daniel Bae



**TFAWS**  
LaRC 2019

Thermal & Fluids Analysis Workshop  
TFAWS 2019  
August 26-30, 2019  
NASA Langley Research Center  
Hampton, VA



# Outline



- Introduction
- MLI Performance Behavior
- Literature
- Application to TD
- Additional Topics: IMLI, Multi-netting, Silk



## Why Study MLI?



- Published  $\epsilon^*$  values vary wildly
- $\epsilon^*$  values depend on temperature and L'Ralph has wide range of temperatures
  - 100 K (IR Detector), 180 K (Vis Detector), and 300 K (Main Electronic Box)
  - Predecessors to L'Ralph are running slightly warmer than expected



# L'Ralph Parasitics Ranking (outdated)



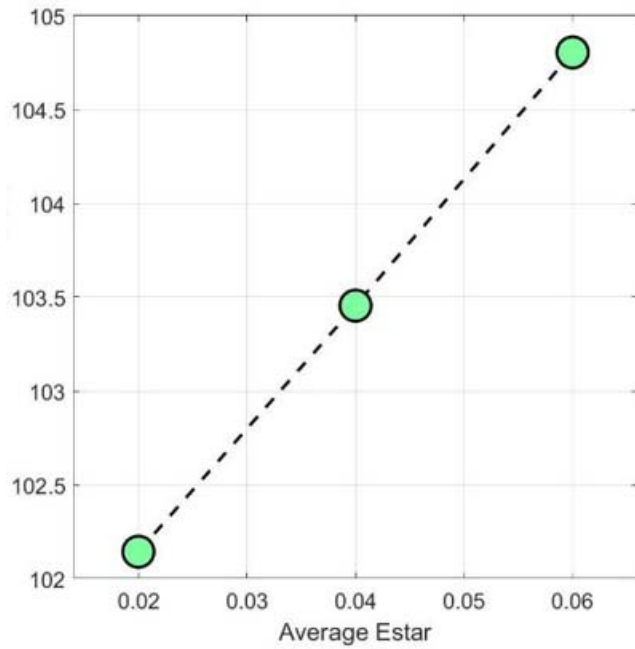
- 1) Multi-layer insulation (MLI) (208 mW)
- 2) Mechanical Supports (90 mW)
- 3) Electrical Harness Parasitics (49 mW)
- 4) IR detector radiative exchange with optics bench interior (35 mW)
- 5) Backloads from L'Ralph's external surfaces (18 mW)



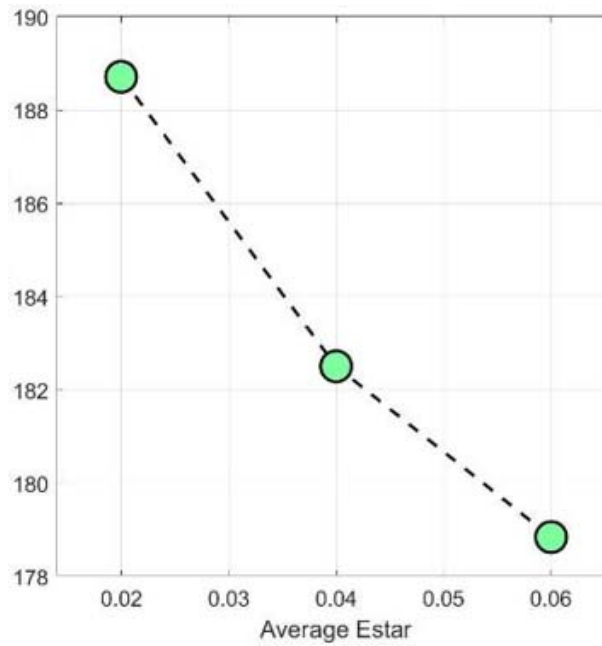
# MLI $\epsilon^*$ Sensitivity



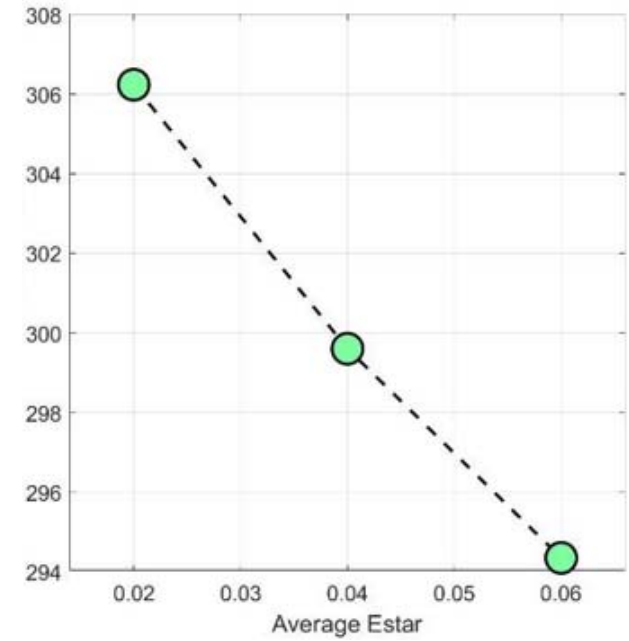
**Cold Detector  
(100 K)**



**Warm Detector  
(180 K)**



**Electronic Box  
(300K)**

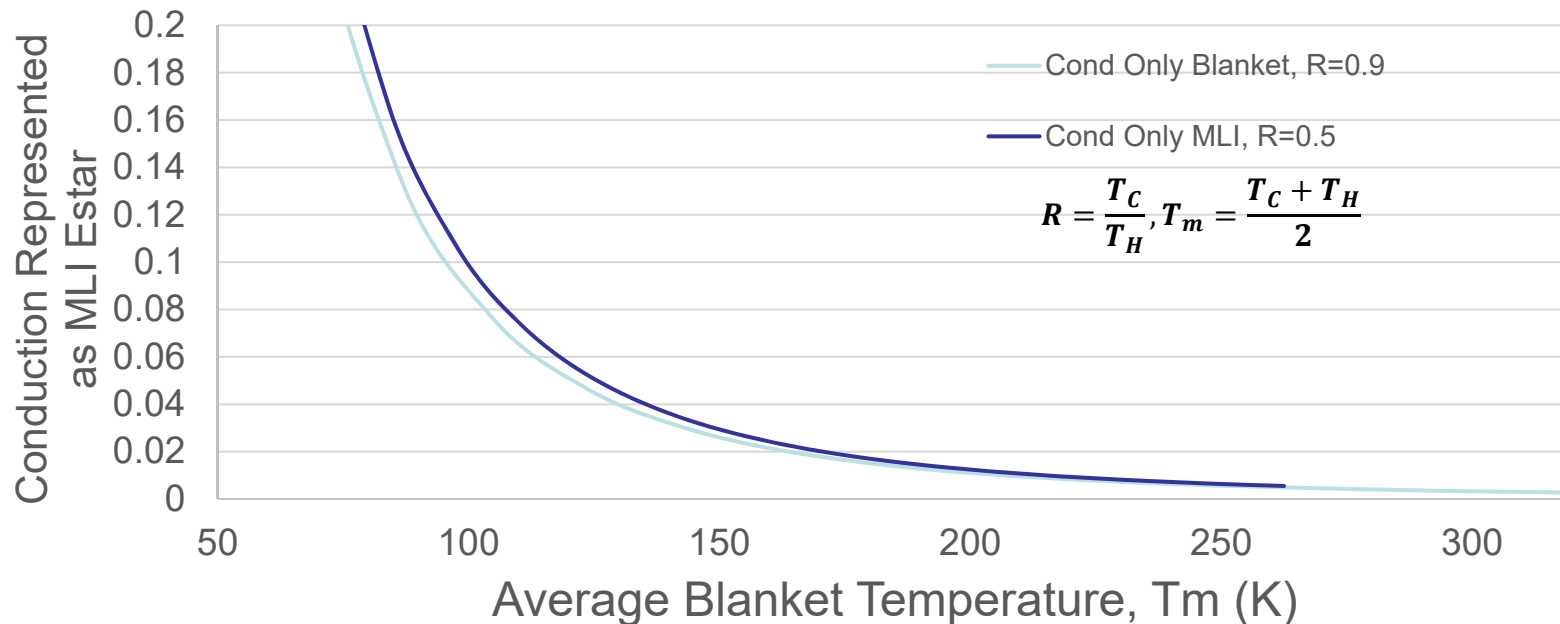




# MLI Behavior



- $\epsilon^*$  can be used to represent total MLI behavior as only a “radiation”
  - $q'' = G_{LIN}(T) \cdot (T_H - T_C) + G_{RAD}(T) \cdot \sigma \cdot (T_H^4 - T_C^4) = \epsilon^*(T) \cdot \sigma \cdot (T_H^4 - T_C^4)$
- If MLI was conduction dominant (i.e.  $G_{RAD}(T) \cong 0$ ) and we were representing the overall MLI effectiveness with  $\epsilon^*$ , we would see an increase in  $\epsilon^*$  as temperature goes down due to lower order behavior of linear conductance
  - $\epsilon^*(T) = \frac{G_{LIN}(T)}{\sigma} \cdot \frac{(T_H - T_C)}{(T_H^4 - T_C^4)}$
  - If we assume  $G_{LIN}(T) \sim constant = 0.025 \frac{W}{m^2K}$ , we would see  $\epsilon^*$  behavior shown below
- The challenge is figuring out how much contribution comes from the linear and radiation terms based on the construction and design of the MLI

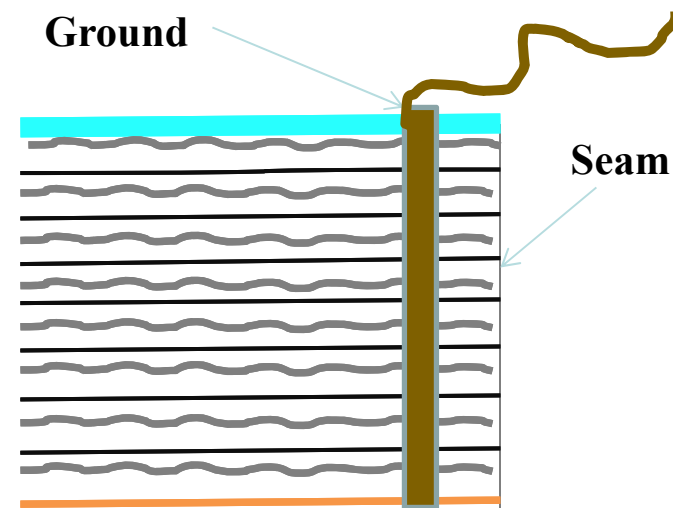




# Blanket Performance Variables



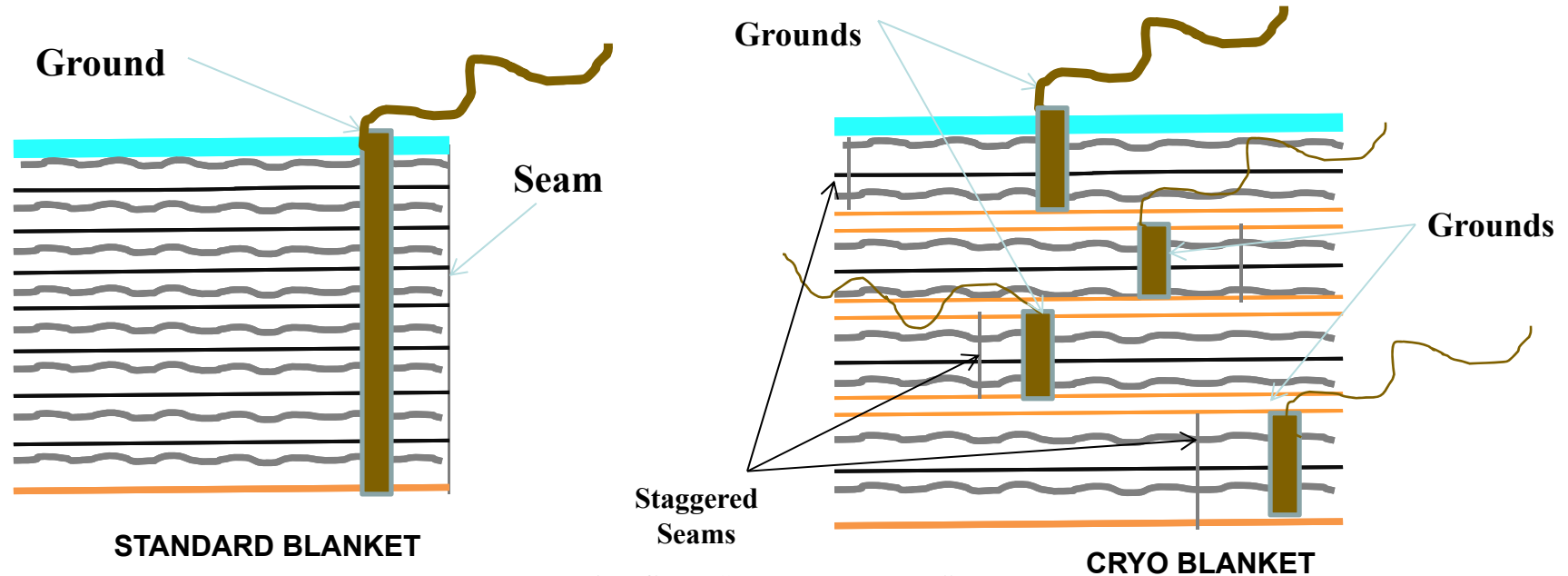
- Emissivity of the materials
- # of blanket layers
- Compression of blanket structure (blanket density)
- Blanket size / footprint
- Thermal spacer resistance
- Gasses within the blankets
- Venting techniques
- Perforations
- # of seams
- Workmanship



STANDARD BLANKET

- Staggered seams to reduce conduction
- Better layer density; more care and more “poofy” construction

Shell method is basically “splitting” the big blanket into layers so that the ground and seam effects are smaller. This is labor intensive but does minimize the heat transfer.

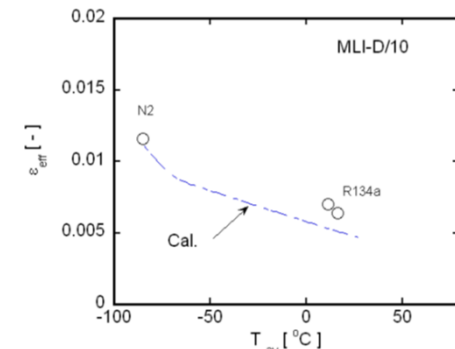
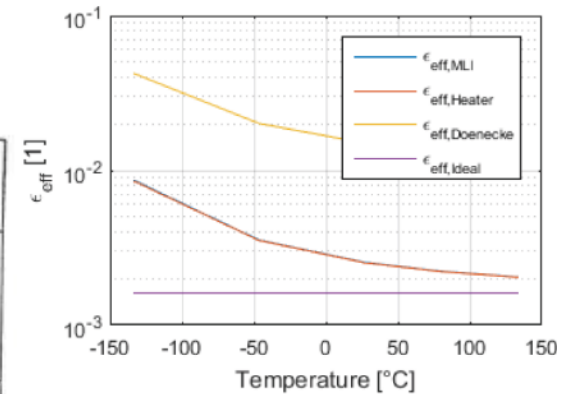
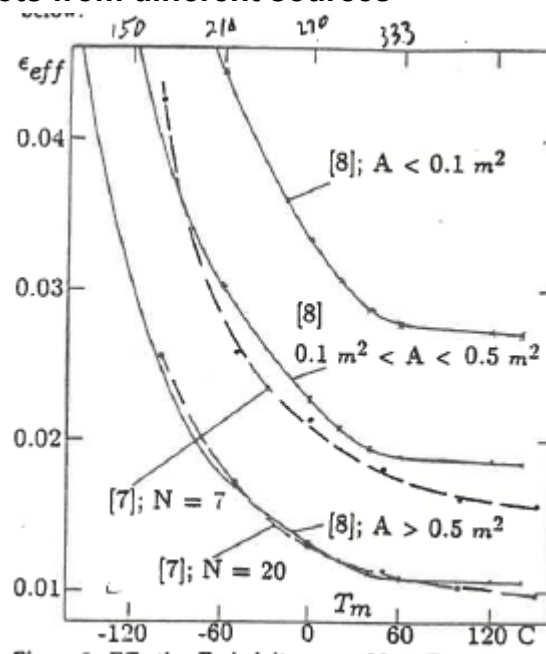
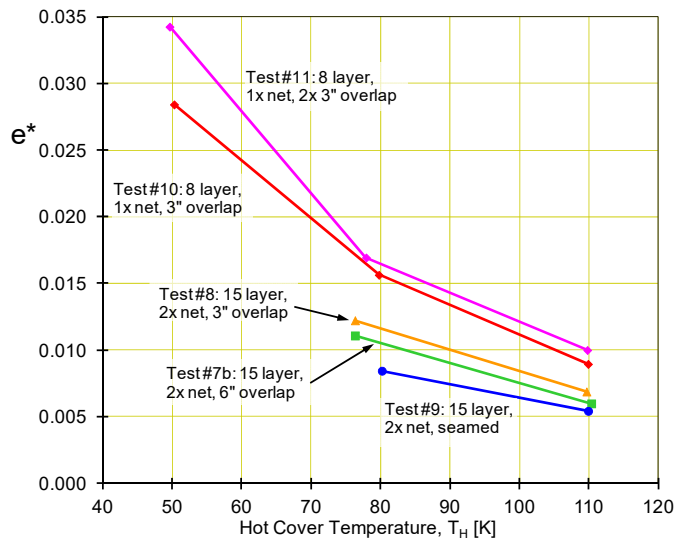


Mosier, Carol, “Thermal Blankets,”  
NASA GSFC, NESC



- MLI performance shows dependence on its operating temperature
  - Keller, 1974 “Thermal Performance of Multilayer Insulations,” Lockheed Martin
  - Doenecke, 1993 “Survey and Evaluation of Multilayer Insulation Heat Transfer Measurements,” SAE Deutsche Aerospace AG
  - Johnson, 2007 “Thermal Performance of Cryogenic Multilayer Insulation at Various Layer Spacings,” Auburn Univ,
  - Kawasaki, 2012 “Temperature Dependence of Thermal Performance in Space Using Multilayer Insulation,” JAXA
  - Rodriguez-Ruiz, 2013 “MLI Effectiveness: Form Fitted, Tented and High/Low  $\epsilon$ ,” GSFC NASA
  - Harpole, 2013 “Cryo MLI Thermal Performance Correlation and Modeling,” JWST, Northrop Grumman
  - Nast, 2014 “Multilayer Insulation Considerations for Large Propellant Tanks,” LM, NASA
  - Ross, 2015 “Quantifying MLI Thermal Conduction in Cryogenic Applications from Experimental Data,” JPL
  - Tiedemann, 2016 “Correlation of MLI Performance Measurement with a Custom MATLAB Tool,” HPS GmbH, Germany
  - And more...

Various  $\epsilon^*$  vs temperature plots from different sources





# Various MLI Correlations



Since we like to think of MLI in terms of  $\epsilon^*$ , the following correlations have been rearranged in the form of  $\epsilon^*$

- Lockheed 1974 -----
  - $$\epsilon^* = \frac{C_s(\bar{N})^{2.56} T_m}{\sigma(N_s+1)} \cdot \frac{T_H - T_C}{T_H^4 - T_C^4} + \frac{C_r \epsilon_{RT}}{\sigma N_s} \cdot \frac{T_H^{4.67} - T_C^{4.67}}{T_H^4 - T_C^4}$$
    - $C_s = 8.95 \cdot 10^{-8} \dots C_r = 5.39 \cdot 10^{-10} \dots \sigma = 5.67 \cdot 10^{-8} \frac{W}{m^2 K^4} \dots \bar{N} = \text{layers/cm} \dots N_s = \text{\# of radiation shields}$
    - $T_m = \frac{T_H + T_C}{2} \dots \text{Temperatures in Kelvins} \dots \epsilon_{RT} = \text{Room temperature shield emittance; typically 0.03}$
- Doenecke, 1993 -----
  - $$\epsilon^* = \left( 0.000136 \cdot \frac{1}{4\sigma T_m^2} + 0.000121 \cdot T_m^{0.667} \right) \cdot f_N \cdot f_A \cdot f_p$$
    - $f_N, f_A, f_p = \text{Correction factors for \# of layers, size of MLI blankets and fraction of perforations, respectively}$
- Modified LM 2010, "New Q Eq" -----
  - $$\epsilon^* = \frac{C_s(0.017 + 7.0 \cdot 10^{-6} \cdot (800 - T_m) + 2.28 \cdot 10^{-2} \ln T_m) \cdot (\bar{N})^{2.56}}{\sigma(N_s+1)} \cdot \frac{T_H - T_C}{T_H^4 - T_C^4} + \frac{C_r \epsilon_{RT}}{\sigma N_s} \cdot \frac{T_H^{4.67} - T_C^{4.67}}{T_H^4 - T_C^4}$$
    - $C_s = 2.4 \cdot 10^{-4}$ , all other constants are the same from 1974 version
- JAXA, Kawasaki, 2012 -----
  - $$\epsilon^* = \epsilon_{eff-R} + \frac{H_{MLI} A_{MLI} + C_{Hem} L}{\sigma A_{MLI}} \cdot \frac{(T_H - T_C)}{(T_H^4 - T_C^4)}$$
    - $\epsilon_{eff-R} = 0.0012 \sim 0.0017 \dots H_{MLI} = 0.0044 \sim 0.0062 \dots C_{Hem} = 0.012 \sim 0.016 \dots L = \text{Seam Length: they had 0.45 m seam for 0.28 m}^2$   
Assume  $L = 0.847 \cdot \sqrt{A} [m]$
- Northrop Grummen-LM, JWST equation, 2013 -----
  - $$\epsilon^* = F \cdot \frac{C_{AA}}{\sigma N_G} \cdot \frac{T_H^{2.34} - T_C^{2.34}}{T_H^4 - T_C^4}$$
    - $C_A = 1.18 \sim 1.58 \cdot 10^{-5} \dots F = 4.5 \sim 7.5 \cdot f(T_m \text{ when } T_m > 114K)$ . Multiplication factor to account for seams/penetrations/etc
- Ross, 2015 -----
  - $$\epsilon^* = \frac{k_0 \kappa(T)}{\sigma N_s} \cdot \frac{T_H - T_C}{T_H^4 - T_C^4} + 1.35 \cdot 10^{-3} \frac{1}{\sigma N_s} \cdot \frac{T_H^2 - T_C^2}{T_H^4 - T_C^4}$$
    - $k_0$  spacer thermal conductance per area,  $\sim 25 \frac{mW}{m^2 K}$  for Silk Net ...  $\sim 900$  for Dacron
    - $\kappa(T)$  relative conductivity of spacer material. Unity at room temperature. In the form of  $\kappa(T) = \frac{1122}{T^2 + 1183} + 1$ . Fitted to get the function

**Not a simple problem and many different contributors**



# Plots of High Biased MLI $\epsilon^*$ for LRalph



- Assumptions:

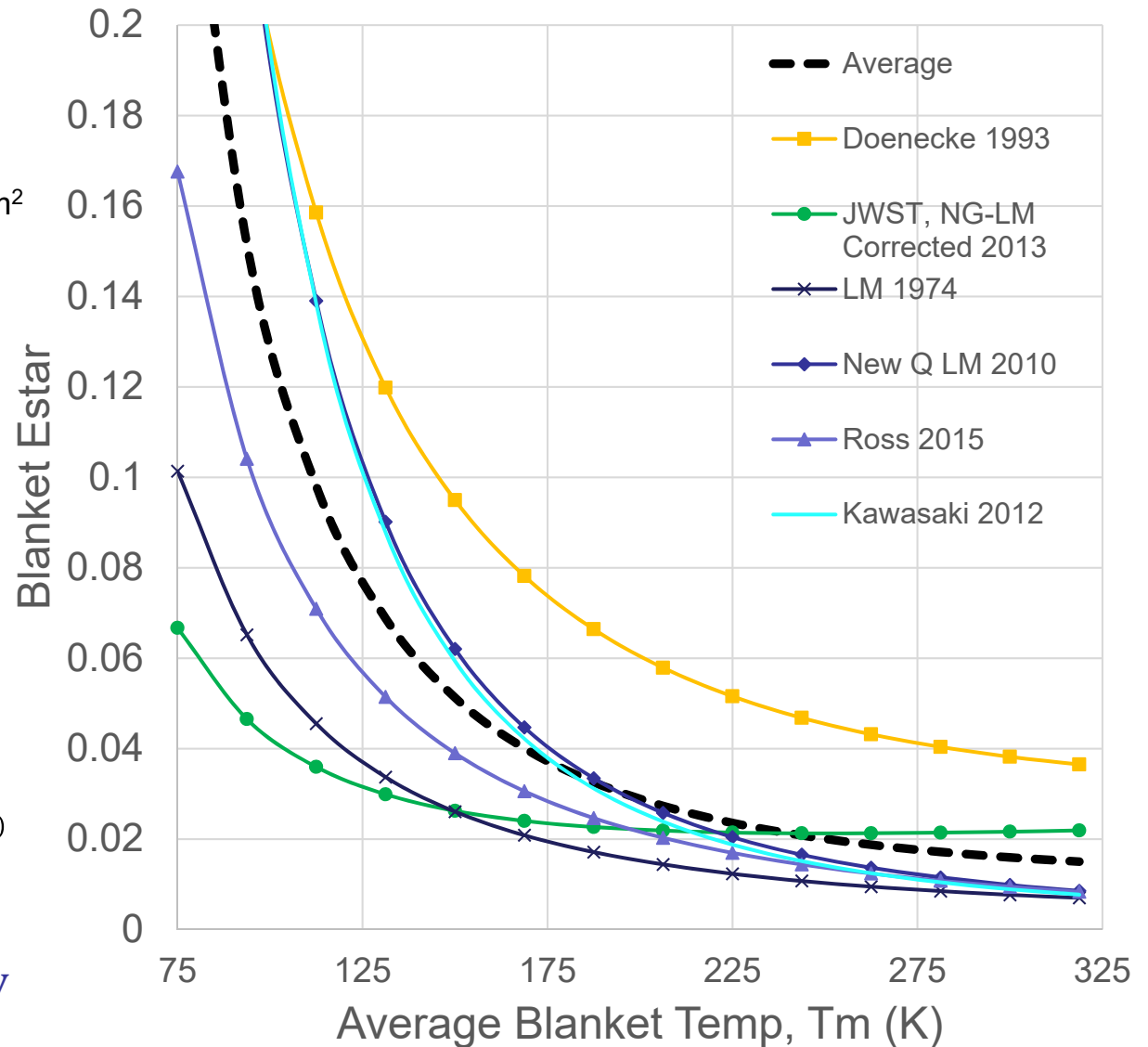
- Overall:

- 13 layers double aluminized
    - Avg MLI area = 0.1 m<sup>2</sup>
    - 40 layers/cm
    - $\frac{T_C}{T_H} = 0.5$

- Correlation Specific:

- LM 1974
      - $\epsilon_{RT} = 0.033$
    - Doenecke
      - $f_N = 1.22$
      - $f_A = 2.36$
      - $f_p = 1.1$
    - JAXA
      - $\epsilon_{eff-R} = 0.0017$
      - $H_{MLI} = 0.0062$
      - $C_{Hem} = 0.016$
    - NG-LM
      - $F = 8 \cdot f_{NG-LM}(T_m)$
      - $C_A = 1.6 \cdot 10^{-5}$

- Note that values are high because L'Ralph is a fairly small instrument





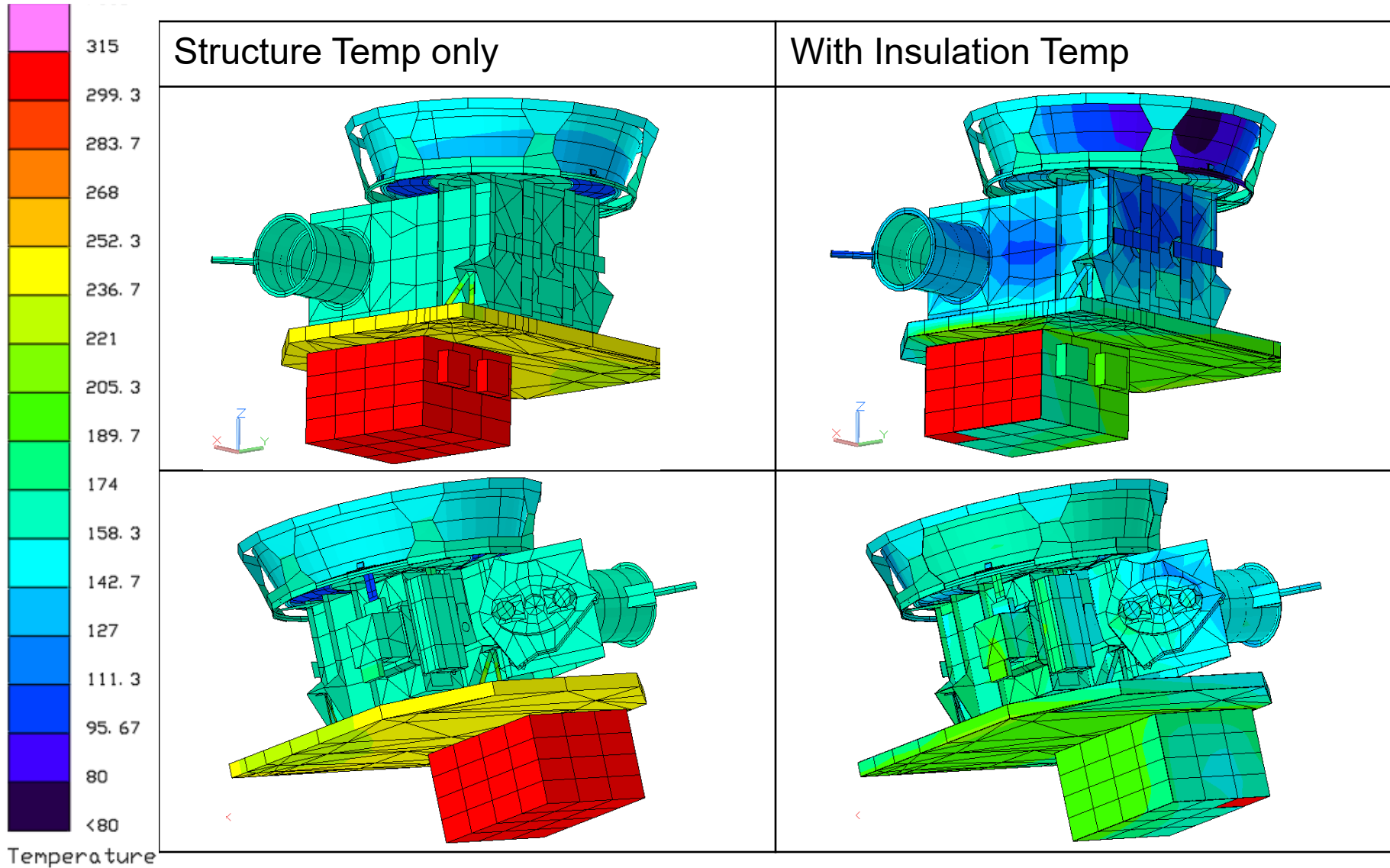
# Application to LRALPH Thermal Model



- There is a wide spread of  $\epsilon^*$  between different correlations
  - Too many factors that contribute to the formulation of  $\epsilon^*$
  - Difficult to choose which correlation to use
- Use average of all the correlations for now until testing results prefer one correlation over another, and bias  $\pm 33\%$  around the average
  - Allows us to capture fairly accurate  $\epsilon^*$  value and behavior as a starting point
- Convert  $\epsilon^*$  to  $K_{eff}$  (i.e.  $K_{eff} = \epsilon^*(T) \cdot \sigma \cdot L_{MLI} \cdot \frac{(T_H^4 - T_C^4)}{(T_H - T_C)}$ )
  - TD cannot accept temperature dependent  $\epsilon^*$  (unless one modifies SINDA input manually), but allows direct temperature dependent conductivity input for insulation connection
  - Note that TD, by default, uses the average temperature between nodes for any temperature dependent conductors
    - Must input K value as a function of average, not hot or cold side temperature
  - We can also use  $4T_m^3 \cong \frac{T_h^4 - T_c^4}{T_h - T_c}$  relation to find  $K_{Eff}$  if only  $\epsilon^*(T_m)$  was available
- Create low, nominal, high  $\epsilon^*$  material properties and apply them based on the insulation heat flow direction in the model
- Based on this method, the thermal model would use approximately the following  $\epsilon^*$  ranges at each temperature zones
  - Note that the actual  $\epsilon^*$  will be determined by the actual structure to insulation mean temperature within the simulation calculations

	Low $\epsilon^*$	High $\epsilon^*$
LEISA (100 K zone)	0.05	0.10
MVIC (180 K zone)	0.03	0.06
MEB (300 K zone)	0.007	0.015

# Instrument at "Hot Position" Insulation vs. Structure Temperature

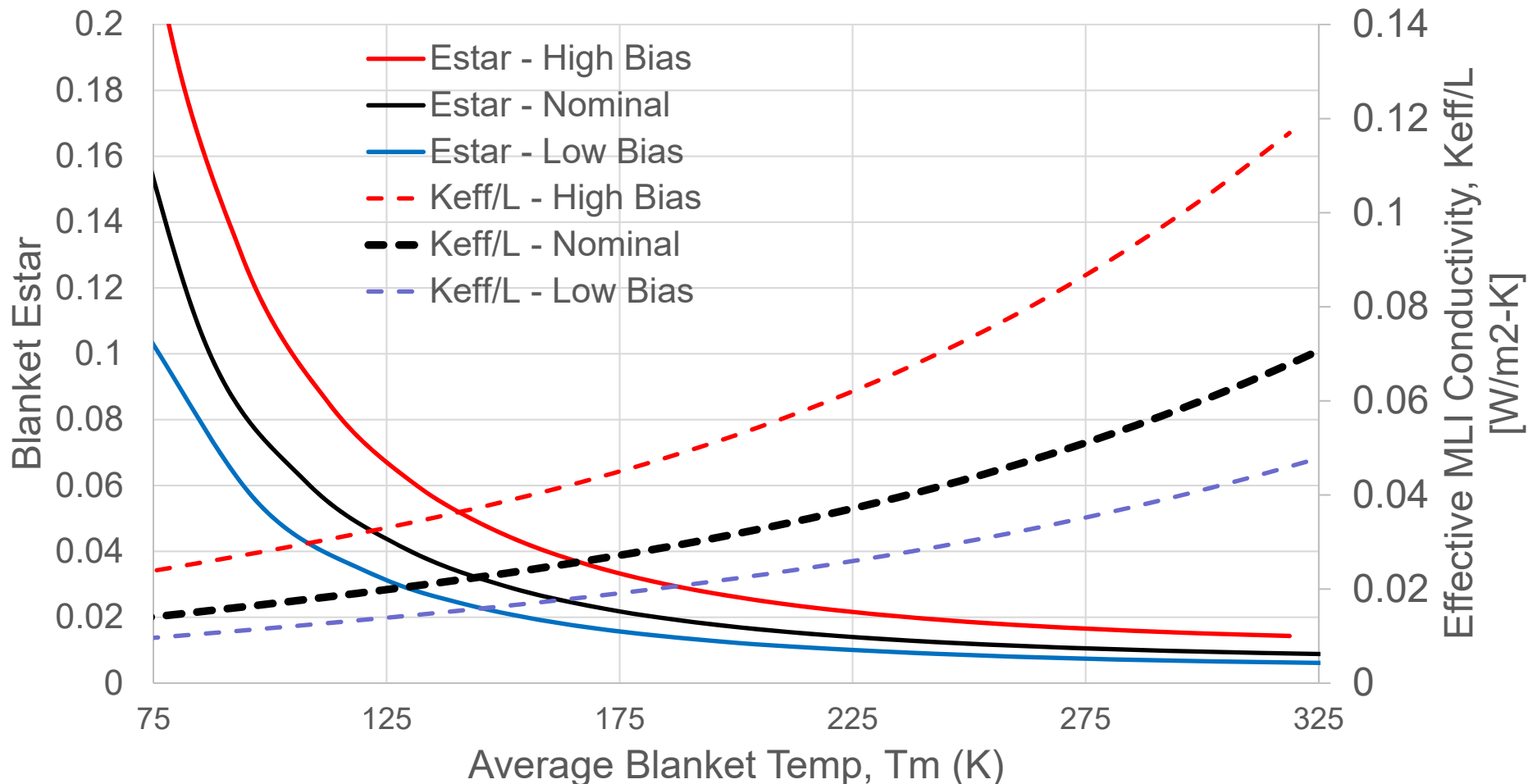




# Temperature Dependent MLI $\epsilon^*$ values

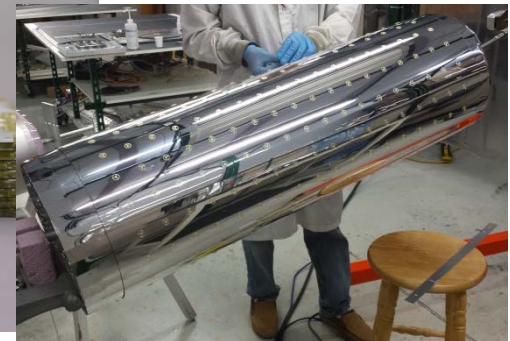
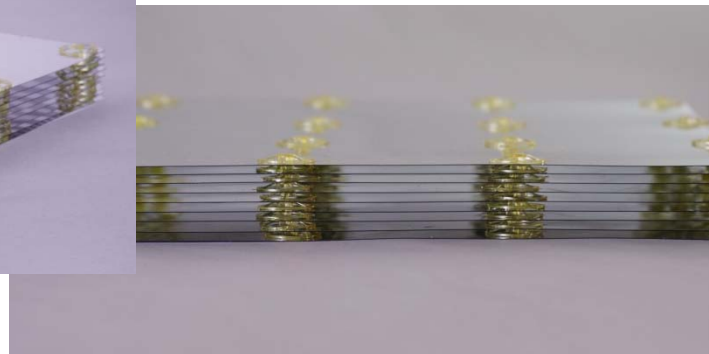
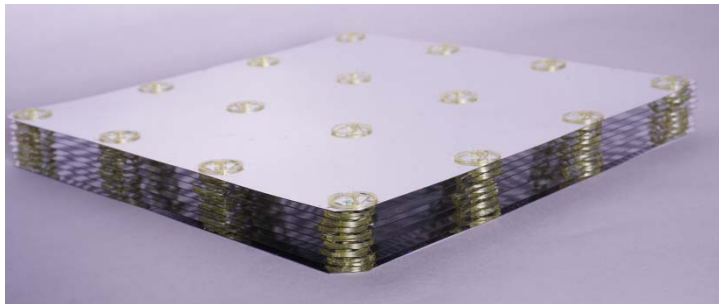
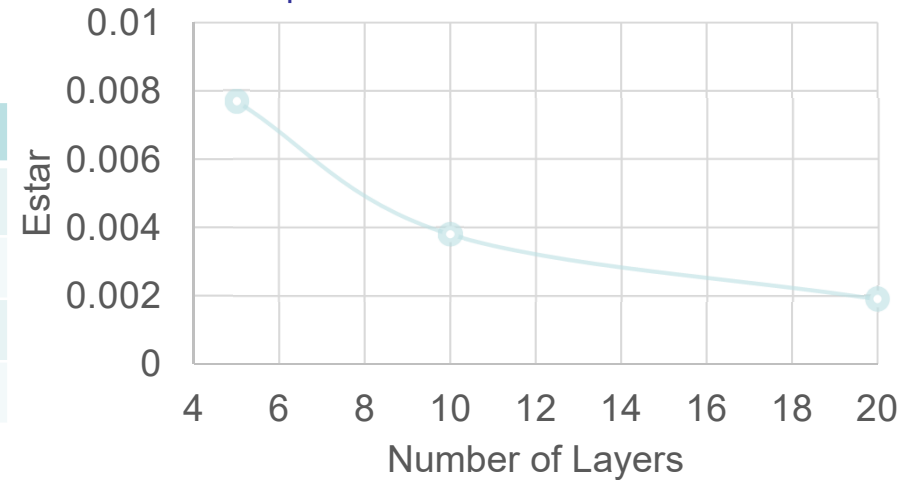


- Plots are based on the average of the correlations shown in an earlier slide
- L'Ralph cryosystem undergoes wide temperature range (between 90 – 180 K)
  - If non temperature dependent value was used, would not capture performance accurately at different temperature zones



- L’Ralph will be using IMLI (DAM separated by low thermal conductance polymer spacers).
  - Aside from grounding paths, edges, and seams, all conductive paths through IMLI are well determined
- Experimental heat flux closely matches modeled IMLI performance.
- Below table shows IMLI estar for 100 and 180K boundary temperatures with conservative 25% degradation allotted for penetrations, etc. Information Quest Thermal Group.

# Layers	Heat Flux (W/m <sup>2</sup> )	Total		
		estar	mass (kg)	Thickness (cm/inches)
5	0.415	0.0077	0.036	0.90/0.36
10	0.205	0.0038	0.073	1.80/0.71
20	0.101	0.0019	0.147	3.61/1.42







# Quest Discrete Spacer Insulation Family

	<b>Application</b>	<b>Status</b>	<b>TRL</b>
<b>Integrated MLI (IMLI)</b>	In space, high vacuum, replaces conventional MLI	Spaceflight. Available.	9
<b>Load Responsive MLI (LRMLI)</b>	One atmosphere to high vacuum, replaces SOFI	Phase 3 completed	5
<b>Load Bearing MLI (LBMLI)</b>	Supports thermal/Broad Area Cooled shields for active cooled systems	Phase 3 completed	6
<b>Vapor Cooled Structure MLI</b>	Active and passive vapor cooling of tank support elements	Phase II complete	5
<b>Multi-Environment MLI (MEMLI)</b>	Operates in environments from space to on- Mars, ISRU surface liquefaction	In Phase II	4
<b>Wrapped MLI (WMLI)</b>	Cryo pipes and plumbing components	Phase II SBIR completed	5
<b>Launch Vehicle MLI</b>	External launch vehicle cryotanks	Phase I SBIR completed	4
<b>Micrometeoroid and Orbital Debris IMLI</b>	High vacuum thermal insulation and MMOD protection	Phase I SBIR completed	4
<b>Vacuum Cellular MLI</b>	Launch vehicles	Early dev	3
<b>Variable Radiator</b>	<b>Spacecraft thermal control</b>	Phase II SBIR in progress	4





# Multi-Netted MLI and Silk vs Dacron Netting



- Multi-netting
  - Instead of single Dacron meshing between layers, multiple can be used to reduce the conductive term
- Dacron vs Silk
  - Netting switched to Dacron around 1970s due to cost of silk
  - Published papers claim that there is a significant difference between the silk and Dacron netting, with silk showing >2x better performance
    - 1974's extensive testing done by LM was done with silk netting

